In situ EC-AFM observation of antimony effect for lead dioxide electrode

Masashi Shiota[a,b,*], Yoshiaki Yamaguchi[a], Yasuhide Nakayama[a],
Nobumitsu Hirai[b], Shigeta Hara[b]

[a]*Yuasa Corporation, 2-3-21 Kosobe-cho, Takatsuki, Osaka 569-1115, Japan*
[b]*Department of Materials Science and Processing, Graduate School of Engineering, Osaka University,*
2-1 Yamadaoka, Suita, Osaka 565-0871, Japan

Abstract

The surface morphologies of lead dioxide layers, which were formed on a pure lead substrate and the Pb–Sb a (100 ppm–3%) alloy substrate, were directly observed with the electrochemical atomic force microscope (EC-AFM) in 1.250 g/cm^3 sulfuric acid electrolyte and then they were analyzed with X-ray diffraction (XRD). The particle size of the lead dioxide became significantly smaller with the increase of the amount of antimony in the substrate alloy. From this result, it was considered that such small particle size serves to increase the reaction area of the positive electrode and the total electrical contact area between the positive active material (PAM) particles. Also, the interface resistance between grid and the PAM can become lower, if the density of the corrosion layer formed around the grid were to be higher for the small particles. By XRD analysis, it was found that the inter-atomic distance of the lead dioxide on the Pb–3 wt.% Sb alloy substrate shrank compared to that on a pure Pb substrate.
© 2002 Elsevier Science B.V. All rights reserved.

Keywords: In situ observation; EC-AFM; Premature capacity loss; Lead–acid battery; Lead dioxide electrodes; Pb–Sb alloy

1. Introduction

For many years Pb–Sb alloys have been used to produce the positive grid of flooded lead acid batteries. Water loss from such batteries has been high, because antimony from the positive grid can migrate through the electrolyte and be deposited on the surface of the negative plate, where it lowers the over-potential for hydrogen evolution [1].

To avoid such harmful effects of antimony, Pb–Ca–(Sn) alloys have been adopted, in some designs, for the grids of lead-acid batteries. Using such an antimony-free positive grid, however, can make the cycle life performance of the positive plate reduce rapidly. This phenomenon is named premature capacity loss (PCL). It has been explained that PCL is caused by the deactivation of positive active material (PAM) during charge/discharge cycle [2,3] or the formation of a barrier layer at the interface between the PAM and the grid [4,5], when antimony is not present in the positive plate. Therefore, it is important for improvement of battery performance to understand the antimony effect in detail.

Our research group has observed and analyzed the reaction processes, which occur at the electrodes in the lead–acid battery, using an electrochemical atomic force microscope (EC-AFM) [6–10]. This new observation technique is very useful for studying the electrode reactions in detail, because it can observe the electrode in sulfuric acid electrolyte directly. Therefore, we applied the in situ EC-AFM to observe the surface morphology of a lead dioxide electrode, which was made from a Pb–Sb alloy substrate. From the results we obtained new knowledge about the antimony effect on the lead dioxide crystals.

2. Experimental

2.1. EC-AFM equipment

We used an EC-AFM observation unit made by Molecular Imaging Co. with a control unit made by Digital Instruments Co. (model NanoScope IIIa). The EC-AFM cell consists of a PbO$_2$ electrode as a counter electrode and a Hg/Hg$_2$SO$_4$ electrode as a reference electrode. All potentials reported here are referred to this electrode. The electrochemical operations were carried out using a

potentio/galvano stat (model HZ-3000) made by Hokuto Denko Co.

2.2. Sample electrode preparation

Sample electrodes were made by gravity mold casting. Electrodes were 100 mm in length, 20 mm in width and 2 mm in thickness. The alloy compositions we studied were pure lead or Pb–Sb (100 ppm–3%) alloy. The electrode surface was polished with abrasive papers and then buffed with fine Al_2O_3 powder. Next, the electrode surface was polished chemically with a mixed solution of acetic acid and hydrogen peroxide and was wiped finally with ethanol.

The sample electrode was assembled into the EC-AFM cell, and then the cell was filled with 1.250 g/cm^3 sulfuric acid electrolyte. The electrode was reduced by two steps of potential, starting at −1400 mV for 10 min followed by −1200 mV for 10 min, to remove lead sulfates from the surface. After that, a lead dioxide layer was formed on the electrode surface by repeating, 10 times, a potential cycle comprising 1250 mV for 10 min and 950 mV for 30 s. In this paper, reduction capacity corresponds to the total quantity of electricity when the potential was changed from 1250 to 950 mV.

2.3. EC-AFM observation

Each lead dioxide morphology was observed by EC-AFM 2 h after sample preparation. The electrode potential had been maintained at 1250 mV, and the temperature was 25 °C through the whole experiment. After the observation of the lead dioxides, the lead sulfate morphology was observed at 950 mV. The observed time, area and mode for an AFM image were 52 s, 5 μm × 5 μm and deflection mode respectively.

2.4. XRD analysis

In order to confirm the chemical composition and crystal structure of the formed lead dioxide layer on each substrate alloy, X-ray diffraction (XRD) analysis was performed with a model RINT 2500 V made by Rigaku Co. Measured samples were washed with ethanol and dried after the above EC-AFM observation.

3. Results and discussion

3.1. Reduction capacity change during the electrode preparation

Fig. 1 shows the reduction capacity changes during the cycles for lead dioxide preparation on the pure Pb substrate and the Pb–Sb alloy substrate. As the antimony content increases, the reduction capacity became smaller.

3.2. EC-AFM image of the lead dioxide

Fig. 2 shows the EC-AFM images of the lead dioxides formed on pure lead substrate and the Pb–Sb alloy substrate. The particle diameters that were obtained from the typical lead dioxide in Fig. 2 are plotted in Fig. 3, versus antimony contents. In this way, it was found that the particle diameters of the lead dioxide became significantly smaller with increasing antimony content in the substrate alloy. Based on these results, the mechanism that antimony in the positive plate suppresses the PCL phenomenon might be explained, as follows.

In the PAM, a smaller particle size serves to increase the reaction area of the positive electrode and the total electrical contact area between the particles. These increases help to maintain the activity of the PAM.

At the interface between the PAM and the grid, the above AFM images make it possible to suppose that the density of the corrosion layer formed around the grid is high. If so, the interface resistance can become low, but also formation of the barrier layer, which is made of lead sulfate, is suppressed. This is because penetration of the electrolyte into the interface is inhibited by the high-density layer structure.
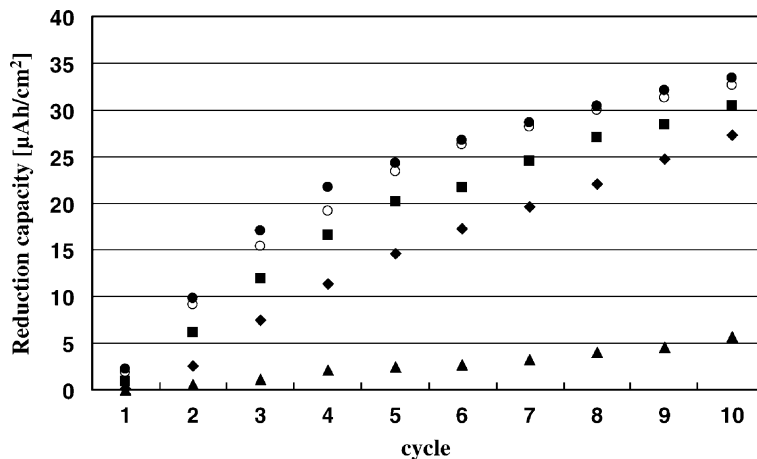

Fig. 1. Reduction capacity changes during cycles for the lead dioxide preparation on pure Pb substrate and the Pb–Sb alloy substrate. (○) Pure Pb substrate; (●) Pb–0.1 wt.% Sb substrate; (■) Pb–0.5 wt.% Sb substrate; (◆) Pb–1 wt.% Sb substrate; (▲) Pb–3 wt.% Sb substrate.
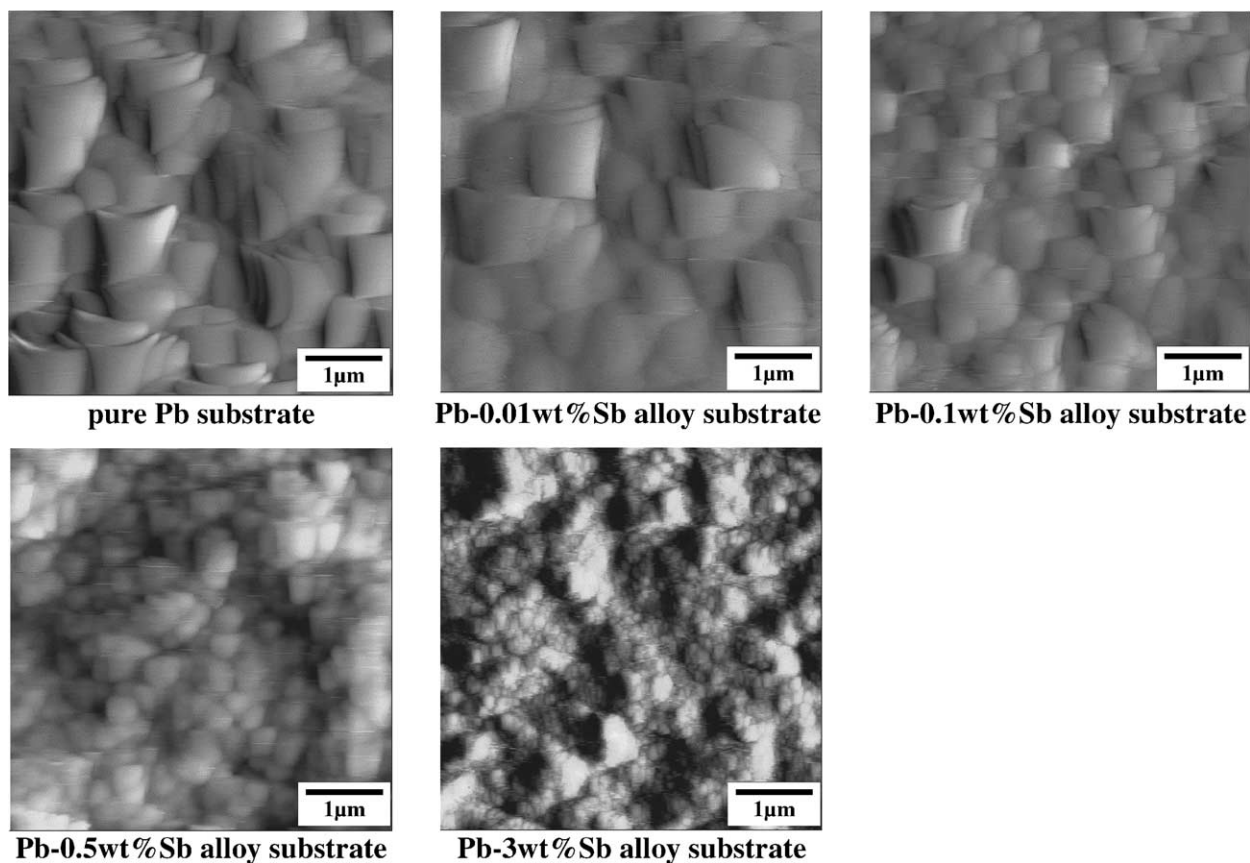
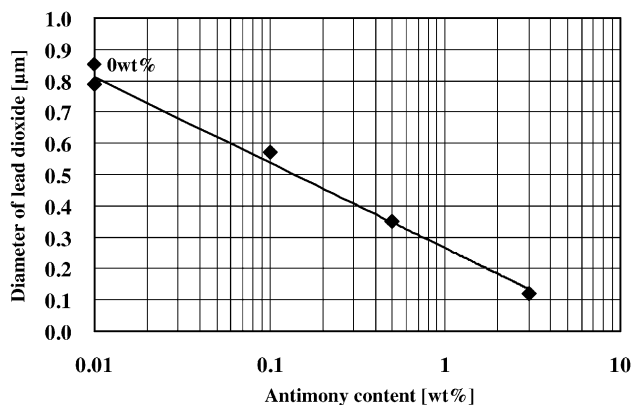Fig. 2. EC-AFM images of the lead dioxides formed on pure Pb substrate and the Pb–Sb alloy substrate.

Fig. 3. Particle diameters of the lead dioxide with the antimony content.

This consideration can be supported and also explained from the result of Fig. 1.

3.3. EC-AFM image of the lead sulfate

Fig. 4 shows the EC-AFM images of the lead sulfates formed on the pure lead substrate and the Pb–3 wt.% Sb alloy substrate. From these two images, it was found that antimony did not affect the lead sulfate morphology Fig. 5.

3.4. XRD result

On XRD measurement, all detected peaks were identified to be lead, α-lead dioxide and β-lead dioxide. As the result of comparison of the diffraction angles of the β-lead dioxide between pure lead substrate and the Pb–3 wt.% Sb alloy

Table 1
Comparison of the diffraction angle of β-PbO$_2$

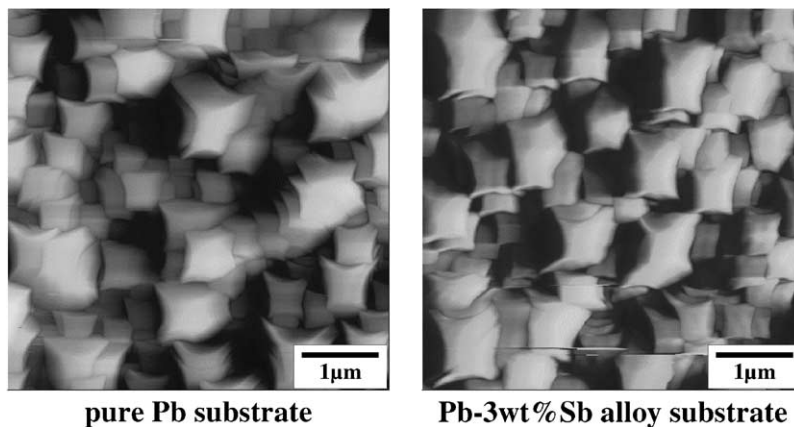|	$2\theta/\theta$											
Miller index	(1 1 0)	(1 0 1)	(2 0 0)	(2 1 1)	(2 2 0)	(0 0 2)	(3 1 0)	(1 1 2)	(3 0 1)	(2 0 2)	(3 2 1)	(2 2 2)
Pb substrate	25.50	32.14	36.38	49.16	52.34	54.30	59.00	60.86	62.26	67.02	74.50	78.56
Pb–3 wt.% Sb substrate	25.58	32.24	36.42	49.26	52.38	54.54	59.12	61.00	62.26	67.36	74.86	78.86

Fig. 4. EC-AFM images of the lead sulfates formed on pure Pb substrate and the Pb–3 wt.% Sb alloy substrate.
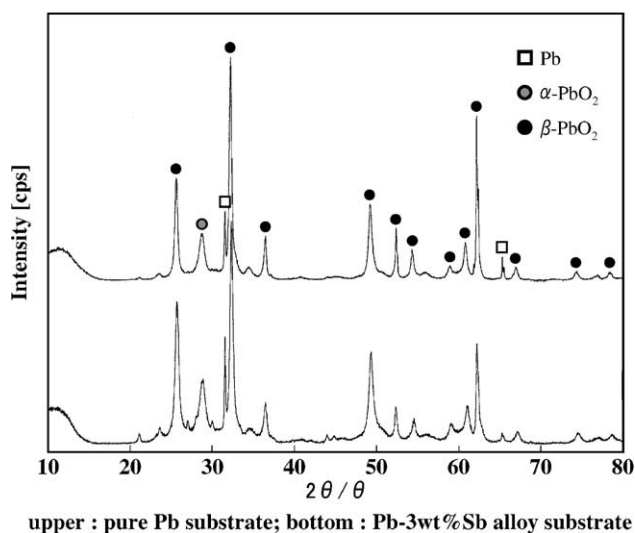

Fig. 5. XRD pattern.

substrate, it was found that the peak on the Pb–3 wt.% Sb alloy substrate shifted to the high angle slightly (Table 1). This means that the inter-atomic distance shrank, and it suggests that the antimony atom was doped into the β-lead dioxide crystal structure; as a consequence of this, it is considered that the particle diameter of the lead dioxide became smaller.

4. Conclusion

We investigated characteristics of the lead dioxide formed on a pure lead substrate and a Pb–Sb alloy substrate using an electrochemical technique, EC-AFM observation and XRD measurement. The experimental results led to the following conclusions related to the antimony effect on the positive plate of the lead–acid battery.

1. As the antimony content of the substrate increases, the reduction capacity during oxidation/reduction cycles for the electrode preparation became smaller.

2. It was found by EC-AFM observation that the particle diameters of the lead dioxide became significantly smaller with increasing antimony content in the substrate alloy. It was considered that this effect of antimony suppresses the PCL phenomenon.
3. The inter-atomic distance of the lead dioxide on the Pb–Sb alloy substrate shrank compared to that on the pure lead substrate.

In these ways antimony affected the electrochemical reaction and the morphology of the lead dioxide significantly. These observations can be related to the performance of the positive electrode in the lead acid battery. Because the EC-AFM is a very useful technique to observe the lead–acid battery's reactions, we would like to clarify the antimony effect in detail by using this technique.

References

[1] B. Culpin, D.A.J. Rand, J. Power Sources 36 (1991) 415.
[2] D. Pavlov, J. Power Sources 48 (1994) 179.
[3] A.F. Hollenkamp, K.K. Constanti, M.J. Koop, L. Apăteanu, M. Calábek, K. Micka, J. Power Sources 48 (1994) 195.
[4] D. Pavlov, E. Bashtavelova, J. Electrochem. Soc. 133 (1986) 241.
[5] A. Winsel, E. Voss, U. Hullmeine, J. Power Sources 30 (1990) 209.
[6] Y. Yamaguchi, M. Shiota, Y. Nakayama, N. Hirai, S. Hara, J. Power Sources 85 (2000) 22.
[7] Y. Yamaguchi, M. Shiota, Y. Nakayama, N. Hirai, S. Hara, J. Power Sources 93 (2001) 104.
[8] M. Shiota, Y. Yamaguchi, Y. Nakayama, K. Adachi, S. Taniguchi, N. Hirai, S. Hara, J. Power Sources 95 (2001) 203.
[9] Y. Yamaguchi, M. Shiota, Y. Nakayama, N. Hirai, S. Hara, J. Power Sources 102 (2001) 155.
[10] I. Ban, Y. Yamaguchi, Y. Nakayama, N. Hirai, S. Hara, J. Power Sources 107 (2) (2002) 167.